weight dependence of the measured thickness of the adsorbed polystyrene layer with that of the average thickness of the adsorbed layer calculated from the concentration profile in the adsorbed polymer chain derived by de Gennes. We found the exponent to be in good agreement with the theoretical calculation of de Gennes.

Acknowledgment. M.K. is pleased to express his thanks to Professor P.-G. de Gennes for his encouragement and useful discussion.

Registry No. Polystyrene, 9003-53-6.

References and Notes

(1) Simha, R.; Frisch, H. L.; Eirich, F. R. *J. Phys. Chem.* **1953**, *57*, 584.
(2) Hoeve, C. A. J. *J. Chem. Phys.* **1966**, *44*, 1505.
(3) Silberberg, A. *J. Chem. Phys.* **1968**, *48*, 2835.
(4) (a) Scheutjens, J. M. H. M.; Fleer, G. J. *J. Phys. Chem.* **1979**, *83*, 1619. (b) *Ibid.* **1980**, *84*, 178.
(5) Stromberg, R. R.; Tutas, D. J.; Passaglia, E. J. *J. Phys. Chem.* **1965**, *69*, 3955.
(6) Gebhard, H.; Killmann, E. *Angew. Makromol. Chem.* **1976**, *53*, 171.
(7) Takahashi, A.; Kawaguchi, M.; Hirota, H.; Kato, T. *Macromolecules* **1980**, *13*, 884.
(8) Dejardin, P.; Varoqui, R. *J. Chem. Phys.* **1981**, *75*, 4115.
(9) Klein, J.; Pincus, P. *Macromolecules* **1982**, *15*, 1129.
(10) Forsman, W. C.; Hughes, R. E. *J. Chem. Phys.* **1963**, *38*, 2130.
(11) Roe, R.-J. *J. Chem. Phys.* **1974**, *60*, 4192.
(12) (a) Hoeve, C. A. J. *J. Polym. Sci., Part C* **1970**, *30*, 361. (b) *Ibid.* **1971**, *31*, 1.
(13) (a) de Gennes, P.-G. *J. Phys. (Paris)* **1976**, *37*, 1445. (b) *Ibid.* **1977**, *38*, 426.
(14) Lal, M.; Stepto, R. J. T. *J. Polym. Sci., Polym. Symp.* **1977**, *No. 61*, 401.
(15) Jones, I. S.; Richmond, R. *J. Chem. Soc., Faraday Trans. 2* **1977**, *73*, 1062.
(16) (a) de Gennes, P.-G. *Macromolecules* **1981**, *14*, 1637. (b) *Ibid.* **1981**, *15*, 492.
(17) Kawaguchi, M.; Takahashi, A. *J. Polym. Sci., Polym. Phys. Ed.* **1980**, *18*, 2069.
(18) Kawaguchi, M.; Hayakawa, K.; Takahashi, A. *Macromolecules* **1983**, *16*, 631.
(19) Kawaguchi, M.; Takahashi, A. *J. Polym. Sci., Polym. Phys. Ed.* **1980**, *18*, 943.
(20) Takahashi, A.; Kawaguchi, M.; Kato, T. *Polym. Sci. Technol. Ser.* **1980**, *12B*, 729.
(21) de Gennes, P.-G. "Scaling Concepts in Polymer Physics"; Cornell University Press: Ithaca, NY, 1979.
(22) Yamakawa, H. "Modern Theory of Polymer Solutions"; Harper and Row: New York, 1971.
(23) Daoud, M.; Jannink, G. *J. Phys. (Paris)* **1976**, *37*, 973.

Viscoelastic Behavior of Atactic Polypropylene

Daniel L. Plazek and Donald J. Plazek*

Metallurgical and Materials Engineering, University of Pittsburgh, Pittsburgh, Pennsylvania 15261. *Received December 21, 1982*

ABSTRACT: The shear creep and recovery behavior of completely amorphous polypropylene was determined at 14 temperatures between −19 and +71 °C. The resulting compliance curves were reduced to 25 °C with apparent success, indicating thermorheological simplicity, but extensive viscosity measurements indicated a different temperature dependence from that of the recoverable compliance in the softening transition, which precludes such simplicity. The retardation spectrum and other viscoelastic functions have been calculated from the creep and recovery response. The glass temperature was ascertained to be −14 °C, and the molecular weight per entangled unit was found to be 4650. The form of the viscoelastic response in the softening transition was found to be semiquantitatively the same as that of polystyrene and poly(vinyl acetate).

Introduction

Isotactic polypropylene, PP, is an important commercial polymer and as such its physical properties have been investigated extensively. Since it cannot be quenched to the completely amorphous state, only the mechanical response of the partially crystalline material has been measured.[1-8] Most of the measurements were made with a continuously varying temperature and a constant frequency or a slowly varying natural frequency of free oscillation or vibration. A few bona fide viscoeleastic studies have been made on partially crystalline polypropylene which was predominantly isotactic. Maxwell and Heider[9] measured the complex dynamic elongational modulus over 5 decades of frequency (10^{-3}–10^{2} Hz) at 11 temperatures between 30 and 110 °C. The results showed the polycrystalline material to be thermorheologically complex; at least three different groups of loss mechanisms were observed.

Earlier, Faucher reported[10] elongational stress relaxation moduli ($E(t)$) measured at times from 10 to 2000 s on highly crystalline isotactic PP at 18 temperatures from −67 to +140 °C. His relaxation spectrum obtained from a reduced modulus curve also indicated three sets of viscoelastic mechanisms. He also presented $E(t)$ curves measured at 14 different temperatures from −67 to +50 °C on a sample of "amorphous" polypropylene. This sample was an ethyl ether extract of a polypropylene of low-crystallinity content. This predominantly amorphous material was estimated from its density of 0.856 g/cm^3 to be about 8% crystalline. The density ρ (25 °C) for completely amorphous PP is 0.850 g/cm^3.[11] The softening dispersion peak of the amorphous component dominates the relaxation spectrum H of this material. However, the crystalline fraction prevents viscous relaxation, corresponding to the flow or permanent deformation that one would observe in a creep experiment. Hence, H does not drop off rapidly toward zero at long times as it does for viscoelastic fluids. Instead relaxation mechanisms are found over the entire measured reduced time-scale range.

Creep measurements have also been made on samples of PP with high and low degrees of crystallinity by Hideshima,[12] but, unfortunately, only the time-scale shift factors were reported. The principal goal in his report was to explain the wide range of glass temperature (T_g) values (−35 to +7 °C) that have been reported in the literature.[2-8,13-17] Natta et al.[13] interpreted the volume–temperature curves of a number of polypropylenes with varying tacticities to all show a T_g break at −35 °C. Hideshima concurred that such breaks are present but that alternate approximately linear portions of the volume–temperature

0024-9297/83/2216-1469$01.50/0

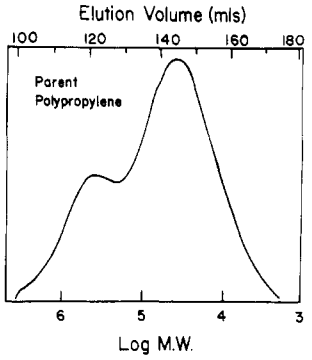

Figure 1. Gel permeation chromatography curve of low-crystallinity polypropylene as received. The solvent used at Hercules was trichlorobenzene.

curve would intersect at about −20 °C, which would agree with the low-temperature point of departure of the shift factor data from a Williams–Landel–Ferry (WLF) equation[18] fit of most of the data. This departure indeed reflects a greater than equilibrium specific volume of the material at the lower temperatures.[19] Hideshima's most amorphous PP was an *n*-heptane extract of highly crystalline material. Since heptane is a better solvent than ethyl ether[20-22] for PP, his sample was most likely more crystalline than that of Faucher.

Polypropylenes that were completely amorphous, i.e., sufficiently atactic, have been prepared and fractionated so that dilute solution properties and molecular weight relationships to the intrinsic viscosity could be established.[23,24] However, the time-dependent properties of a linear polypropylene that is completely amorphous and hence a viscoelastic fluid apparently have not previously been determined. The current investigation was therefore undertaken to determine the softening dispersion of amorphous polypropylene in terms of the shear creep compliance ($J(t)$ (cm^2/dyn)) and its temperature dependence.

Experimental Procedures

Materials. The characterized polypropylene from which the atactic completely amorphous viscoelastic liquid was extracted was generously supplied to us by J. B. Class of Hercules Inc. It was a research sample with a low degree of crystallinity, 5.9% by differential scanning calorimetry (DSC). Infrared analysis indicated that it was 97% atactic.[25] Gel permeation chromatography (GPC) yielded a number-average molecular weight (M_n) of 25 900 and a weight-average molecular weight (M_w) of 205 000. The GPC curve, indicating a bimodal molecular weight distribution, is shown in Figure 1. The above data were obtained at Hercules Inc.

Approximately 10 g of the flexible translucent sheet of material was heated in 1 L of boiling *n*-heptane overnight. Twenty-two milligrams of an antioxidant (Santanox, 4,4-thiobis[6-*tert*-butyl-*m*-cresol]) was added to inhibit the thermal oxidative degradation of the PP. The mixture was allowed to cool to room temperature, where much of the crystallizable material precipitated, forming a stable cloudy suspension. Kinsinger[24] alludes to "earlier separation difficulties", which we found as an unfilterable, difficult to centrifuge suspension. The precipitate particles obviously contained dangling amorphous chains, which caused them to be sticky. Filter media were almost immediately clogged. Preparative centrifugation at 10 000 rpm for several hours resulted only in partial sedimentation. Convenient successful separation was achieved with the slow addition of acetone until an increase in turbidity was noted. Simultaneous final precipitation with initial coacervation yielded a flocculent precipitate that settled within minutes to yield a completely clear supernatant. Filtering through coarse media was fast and effective. Our mixed solvent was of poorer solvent quality than a Flory (Θ) solvent. It is our opinion that no crystallizable polymer can be maintained in solution in such a poor solvent. Further addition of acetone to the clear supernatant resulted in continued coacervation; i.e., a cloud point was achieved, and the separated concentrated phase coalesced and settled overnight. The ensuing fractions were clear viscoelastic liquids.

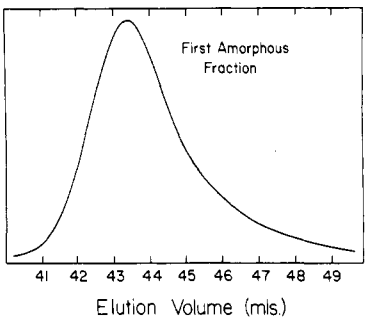

Figure 2. Gel permeation chromatography curve of the first completely amorphous fraction of polypropylene. Solvent was tetrahydrofuran at 25 °C.

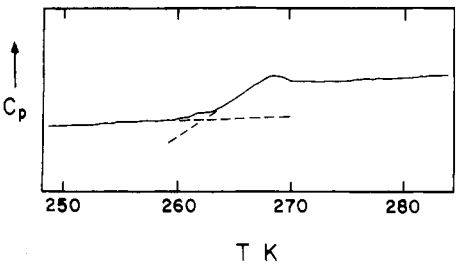

Figure 3. Heat capacity of amorphous polypropylene as a function of temperature obtained by differential scanning calorimetry with a heating rate of 10 °C/min.

The first completely amorphous fraction was studied. GPC characterization was carried out on a Waters 150 instrument by L. J. Fetters at the Institute of Polymer Science, University of Akron. The resulting curve obtained from a solution in tetrahydrofuran at 25 °C is shown in Figure 2. The number-, weight-, and *z*-average molecular weights are 6.0×10^4, 1.05×10^5, and 1.44×10^5, respectively. The parent polymer had a heterogeneity index (M_w/M_n) of 7.9_3, whereas the value for the first amorphous fraction is 1.7_5. The low molecular weight peak of the parent indicated in Figure 1 is 3.9×10^4. It is therefore apparent that our separation procedure has yielded a fraction near the low molecular weight peak and that nearly all of the species populating the high molecular weight peak have been lost. The M_z/M_w ratio for the fraction, 1.3_7, suggests as does the GPC curve that there is little of a high molecular weight tail.

Creep Measurements. Torsional creep and recovery measurements were carried out with two different magnetic-bearing apparatuses,[26] with the specimens in the form of cylinders held between flat circular platens by self-adhesion. Nominal $^1/_8$- and $^1/_4$-in-diameter samples were measured. Checks made with torques ranging up to 25-fold indicated that our measurements were in the realm of linear viscoelastic behavior. In addition to viscosities obtained from creep measurements in the terminal[26] or near-terminal[27] region of response, viscosities were determined from a series of measurements, where following the attainment of steady-state creep, the torque was held fixed while the temperature was incrementally varied from +69 to −7 °C.[28] The following equation was used to obtain specific volumes ($\bar{V}$) needed to calculate the shear creep compliance ($J(t)$) values:

$$\bar{v}(T\ °C) = \bar{v}(25\ °C)[1 + \alpha(T - 25)]$$

where $\bar{v}(25\ °C) = 0.8503\ cm^3/g$[21] and $\alpha = 6.2 \times 10^{-4}\ cm^3/(cm^3\ °C)$.[14]

Determination of the Glass Temperature. A Perkin-Elmer Model 2 differential scanning calorimeter was used to determine the glass temperature (T_g) of the completely amorphous PP. A cooling and heating rate of 10 °C min^{-1} and a sensitivity of 1 mcal s^{-1} were used on 3.0 mg of material. The intersection of the base line (below T_g) with the line drawn with the slope at the point of inflection yields a T_g of −11 °C; see Figure 3. We believe, based on earlier comparisions,[29] that this corresponds to a conventional

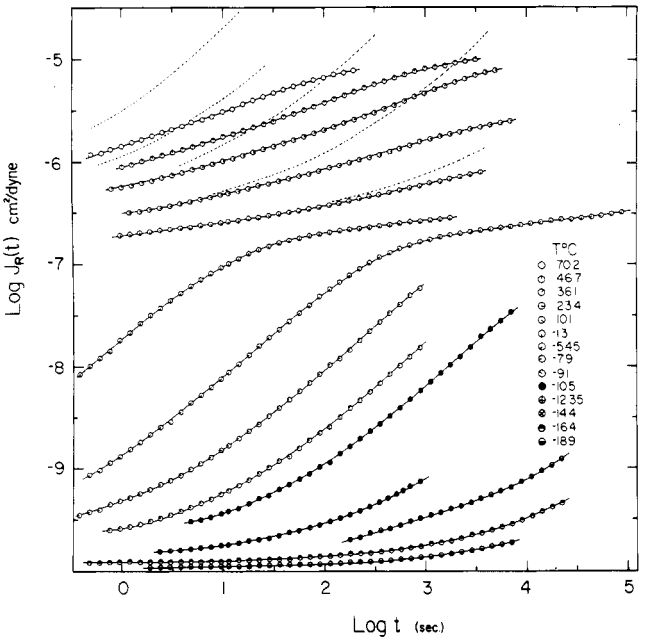

Figure 4. Logarithmic recoverable creep compliance $J_R(t)$ presented as a function of the logarithm of the time of recovery at 14 temperatures as indicated in the key. Dashed lines indicate the measured creep compliance curves $J(t)$ where they differ from the recovery.

dilatometric (1 °C min^{-1} cooling rate) value of −14 °C.

Results and Discussion

Creep and Recovery Compliances. The shear creep compliance ($J(t)$) and recovery ($J_R(t)$) curves are shown in Figure 4. Curves are presented for 14 temperatures from −19 to +70 °C. Where $J(t) > J_R(t)$, the $J(t)$ curves are represented by dashed lines. The response displayed represents the glassy behavior at temperatures below T_g and extends to nearly steady-state terminal behavior at the highest temperatures. Between −5 and +10 °C, the $J(t)$ curves exhibit a rubbery plateau, which is commonly attributed to the presence of a transient network of entangled threadlike molecules. The highest temperature recovery curves indicate an approach to a steady-state recoverable shear compliance J_e^0 of about 1.2×10^{-6} cm^2/dyn.

Temperature Reduction. If the viscoelastic mechanisms contributing to the creep deformation do not change in strength with temperature and all shift along the time scale by the same factor, a_T, the log $J(t)$ curves as functions of the logarithmic time scale do not change their shape with temperature variations. Only their horizontal position changes. Viscoelastic response curves such as $J(t)$ are defined over the entire time scale, and at each temperature only a portion of the response is observed, which depends on the experimental window, which for the reported measurements extends from t = 0.4 s up to 1 day. Therefore, if the above assumptions hold, measurements made at different temperatures will yield an extended reduced curve of response when the curve segments are shifted along the time scale to superpose at an arbitrarily chosen reference temperature T_0. When such a reduction is successful, the material is termed "thermorheologically simple".[30] The reference temperature T_0 was chosen as 25 °C, and all of the compliance curves were simply shifted along the time scale to achieve the superposition seen in Figure 5. No significant departures from successful superposition can be discerned; thus the amorphous polypropylene appears to be thermorheologically simple within our experimental uncertainty. This conclusion is surprising

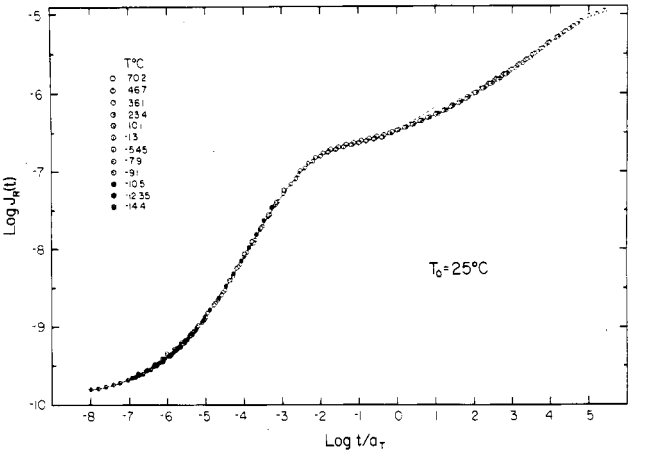

Figure 5. Logarithm of the recoverable shear creep compliance $J_R(t)$ shown as a function of the logarithmic reduced time scale t/a_T. The response is reduced to 25 °C as the chosen reference temperature. Curves below T_g, which are not at equilibrium density, are omitted from this reduced curve.

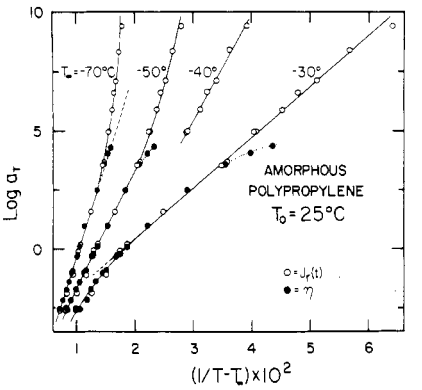

Figure 6. Logarithm of the time-scale shift factors a_T vs. the reciprocal temperature difference $1/(T - T_\infty)$. T_∞ values are shown next to the curves for which they were used. Open-circle data points were obtained from the reduction shifts of the $J_R(t)$ curves. Filled-circle data points are values of $\eta(T$ °C$)/\eta(25$ °C).

since the vinyl polymers polystyrene (PS)[26a] and poly(vinyl acetate) (PVAc)[31,32] are not completely thermorheologically simple. The softening dispersion has a different temperature dependence of time-scale shift ($a_{T,S}$) from that of the terminal dispersion ($a_{T,W}$), which is experimentally identical with that of the viscosity $a_{T,\eta}$.

Since it is possible to obtain apparently successful but fallacious superposition,[26a] it was desired to test further for this simplicity. In addition, it is of interest to ascertain whether the temperature dependence or dependences are describable by the Williams–Landel–Ferry (WLF) equation,[33,34] which is interpreted as an intrinsic dependence of the rate of irreversible processes on the fractional free volume available. The WLF equation is equivalent to the explicit free volume Doolittle equation.[35]

The set of shift factors obtained from the temperature reduction of the log $J_R(t)$ curves (open circles) is plotted in Figure 6 as a function of the reciprocal temperature difference $(T - T_\infty)^{-1}$. The effect of different choices for the adjustable characterizing parameter T_∞ is illustrated. This plot is a test for the applicability of the Vogel–Fulcher–Tamman–Hesse[36-38] (VFTH) equation, which is an alternative form of the WLF equation.

$$a_T \simeq \eta(T)/\eta(T_0) = \frac{A}{\eta(T_0)} e^{C/(T-T_\infty)} \qquad (1)$$

The viscosity at the reference temperature is $\eta(T_0)$, and A, C, and T_∞ are characterizing parameters. All of the shift

Table I
Temperature Dependencies (T_0 = 25 °C)

T, °C	log η	log $a_T(\eta)$	log $a_T(J_w)^a$	log $a_T(J_s)^b$
70.2	5.72_1	−2.53	−2.55	
68.4	5.69_4	−2.56		
59.4	6.08_0	−2.17		
50.4	6.53	−1.72		
46.7	6.56_0	−1.69	−1.85	
45.0	6.85_3	−1.40		
38.9	7.23_1	−1.02		
36.1	7.34_9	−0.90	−1.09	
25.0	(8.25_0)	0.00	0.00	
29.4	7.93_4	−0.32		
29.2	7.93_9	−0.31		
37.1	8.04_2	−0.21	−0.07	
23.4	8.34_4	0.09	0.20	
15.2	9.22_5	0.98		
10.2			1.65	
4.5	10.72_0	2.47		
−1.3			3.54	
−1.9	11.83_8	3.59		
−2.1			3.71	
−4.8	12.32	4.07		
-5.4_5				4.97
−7.0	12.61	4.36		
−7.9				5.90
−9.1				6.64
−10.5				8.39
−14.4				9.39

[a] Values determined from the terminal dispersion. [b] Determined from the softening dispersion.

factors obtained in this investigation are presented in Table I. It is clear that there is no value of T_∞ that will satisfy the α_Ts obtained from $J_R(t)$. The low-temperature data require a value in the neighborhood of −70 °C and the high-temperature data need a value near −30 °C. Two possible reasons exist for the lack of a complete fit to the data. This type of free volume equation simply may not be the correct representation for the data. A second possibility is that the data may reflect two or more different temperature dependences, each of which is describable with a free volume equation.

The shift data obtained do not distinguish between these two possibilities. Therefore a separate series of viscosity determinations was made following the attainment of steady-state flow near 70 °C. With the constant torque maintained, the temperature was changed and equilibrated at over a dozen temperatures down to −7.0 °C with an attendant increase of the viscosity of 10^6-fold. The determination at −4.8 and −7.0 °C overlap with the a_T values obtained from softening dispersion shifts and clearly indicate significantly smaller values of a_T than those obtained from the softening dispersion. It is concluded that the behavior of PP is similar in the viscoelastic response between the glassy level and steady state to that of PS and PVAc in that two temperature dependences are present. The apparently successful reduction in Figure 5 is therefore misleading. Protracted creep or recovery measurements in the neighborhood of 0 °C would presumably reveal a lack of reducibility and hence a lack of complete thermorheological simplicity.

Within the uncertainty of our data, two VFTH equations hold:

$$\log a_T = A' + 446(T + 40\ °C)^{-1} \quad (2)$$

for the softening dispersion and

$$\log a_T = A'' + 640(T + 60\ °C)^{-1} \quad (3)$$

for the viscosity and the terminal dispersion. The constants A' and A'' are determined with a choice of reference temperature where log a_T = 0. If the behavior of the PP is qualitatively similar to that of PVAc, eq 3 will hold even at temperatures approaching T_g whereas eq 2 will not.[32]

It should be noted that the $J(t)$ curves obtained below the measured T_g were omitted from the reduction analysis since the observed shift factors are not unique because of the lack of attainment of an equilibrium density.

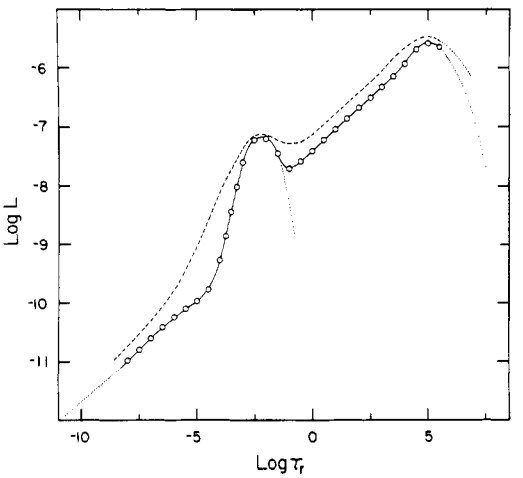

Figure 7. Logarithm of the distribution function of retardation times (the retardation spectrum) L shown as a function of the logarithm of the reduced retardation time τ_r. Dotted lines are extrapolations and the dashed line is log $(J'' - 1/\omega\eta)$, where $\tau_r = 1/\omega_r$. ω_r is the reduced circular frequency in radians s^{-1}. Units of L are cm^2/dyn.

Derived Viscoelastic Functions. Retardation Spectrum. The reduced $J_R(t)$ curve from Figure 5 was used to obtain the distribution function of retardation times, $L(\ln \tau)$ (frequently called the retardation spectrum).[33] An iterative computer program with manual intervention,[29,39] was used to obtain an $L(\ln \tau)$, which upon numerical integration yielded the input data to within ±2%. The relationship used is

$$J_R(t) = J_g + \int_{-\infty}^{+\infty} L(\ln \tau)(1 - e^{-t/\tau})\ d \ln \tau$$

where J_g is the glassy compliance and τ is the retardation time.

The $L(\ln \tau)$ obtained is shown in Figure 7, where the usual features for a moderately high molecular weight linear amorphous polymer are seen. At the shortest times a slope close to $^1/_3$ is observed, which suggests that this region is dominated by Andrade creep.[40-42] Recoverable creep, which is linear with $t^{1/3}$ as in this kind of creep, yields an $L(\ln \tau)$ that is proportional to $\tau^{1/3}$. When a distinct group of loss mechanisms (usually called β mechanisms when found just preceding the softening or α process) is absent, the first departure from the glassy level always seems to be Andrade creep.[43,44] It is not certain whether the slight shoulder in $L(\ln \tau)$ in the neighborhood of log τ = −6.0 is real or an aberration caused by temperature-reduction errors.

When a polymer exhibits a rubbery plateau in the compliance or rigidity functions as does our PP sample, a fairly symmetrical peak is found in $L(\ln \tau)$ following the Andrade region just mentioned. This softening peak indicates the location of the highest population of viscoelastic mechanisms leading to the rubbery compliance J_N. At our chosen reference temperature of reduction T_0 = 25 °C this peak is centered about 6 ms. The terminal or long-time peak is estimated to be at about 1.0×10^5 s. Whereas the shape and magnitude of the terminal peak are strong functions

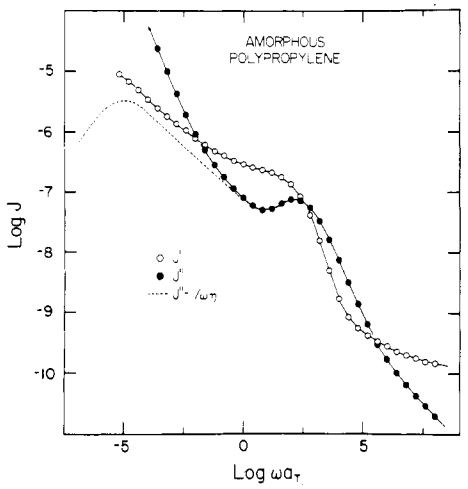

Figure 8. Logarithmic plots of the components of the complex dynamic shear compliance $J^*(\omega)$ of amorphous polypropylene vs. the logarithm of the reduced frequency ωa_T. Open circles are the storage compliance J' and the filled circles are the loss compliance J''. The dashed line represents the nonviscous contribution to the loss compliance, $J'' - 1/\omega\eta$. T_0 = 25 °C.

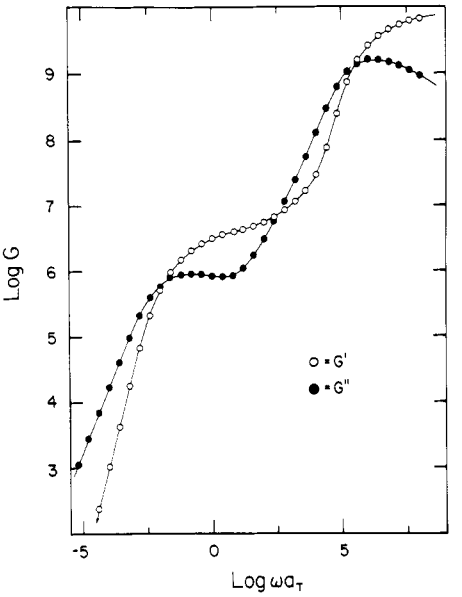

Figure 9. Logarithmic display of the components of the complex dynamic shear modulus $G^*(\omega)$ as a function of the logarithmic reduced circular frequency ωa_T. Open circles are the storage modulus G' values and the filled circles are the loss modulus values G''. The reference temperature of reduction is 25 °C.

of the molecular weight distribution, the softening peak is independent of the molecular weight and its distribution at high molecular weights. Often, the region between the two peaks is a second Andrade creep region,[40,41] which we now believe to be independent of the first Andrade region in the glassy region of response. The slope of the straight-line portion of $L(\ln \tau)$ between the two maxima in Figure 7 has a slope of 0.35, which is a strong indication of the presence of Andrade creep over the 5 decades of time from log t = −1.0 to log t = 4.0.

The softening peak was extrapolated as indicated in Figure 7. The integral under this curtailed $L(\ln \tau)$ is the entanglement network compliance J_N. log J_N was found to be −6.655. Assuming the kinetic theory of rubber-like behavior to be applicable to the transient entanglement network, a molecular weight per entangled unit M_e was determined to be 4650 at T = 298 K from

$$M_e = J_N \bar{\rho} RT$$

where ρ is the density and R is the ideal gas constant. This corresponds to 222 chain backbone atoms per entangled unit.

Dynamic Compliances. The retardation spectrum shown in Figure 7 was used to calculate the components of the complex dynamic shear compliance, $J^*(\omega) = J' - iJ''$, with the usual relations.[33] The storage compliance is J'; J'' is the loss compliance. A computer program employing numerical integration was used to obtain the compliance values.[33] The results of the calculations are seen in Figure 8 as a function of the logarithm of the reduced radian frequency scale; $\omega_r = \omega a_T$ (s^{-1}). The contribution of the viscous deformation $1/\omega\eta$ to J'' can be seen below log ωa_T = 0. The dashed line represents the contribution of the recoverable deformation to J''. The quantity $J'' - 1/\omega\eta$ is the zeroth approximation of the retardation spectrum when it is assumed that $\omega = \tau^{-1}$. To show what such a statement means, log $(J'' - 1/\omega\eta)$ has been plotted against log τ (=−log ω) in Figure 7. The maxima correspond but the $J'' - 1/\omega\eta$ values are greater at all times than L, and its peaks are broader and more diffuse. The position and magnitude of the terminal peaks in the viscoelastic functions L, $J'' - 1/\omega\eta$, and G'' are sensitive functions of the molecular weight distribution in as yet an unknown manner. For polymers with narrow molecular weight distributions it is known that the separation of the two peaks in $L(\ln \tau)$ increases as does the viscosity with the 3.4 power of the molecular weight.[47,48] In addition, since $J_e = (2.5\text{–}3.0)J_N$ for such "monodisperse" polymers, the areas under semilogarithmic plots of $L(\ln \tau)$ are related by the same ratios. Not only does the same molecular weight dependence apply to the separation of the peaks in $L(\ln \tau)$ as to the viscosity but the separation goes to zero at M_c, the same molecular weight where the entanglements start to affect the magnitude of the viscosity. The separation of peaks of the retardation spectrum is a good objective measure of the length of the rubbery plateau. For polymers with heterogeneity indices M_w/M_n larger than 1.02 the terminal peak and the length of the rubbery plateau are greatly enhanced.

The rubbery plateau is seen in the log J' curve at log ωa_T = 0. The features of J' are qualitatively similar to those of $J_R(t)$, as usual where $\omega = t^{-1}$: $J'(\omega) \leq J_r(1/t)$.[33] This inequality becomes more severe with the sensitivity of $J'(\omega)$ to the frequency.

Dynamic Rigidities. The components of the complex dynamic shear modulus, $G^*(\omega) = G' + iG''$, calculated from J^* are shown in Figure 9 as a function of reduced circular frequency; G' is the storage modulus and G'' the loss modulus. The limiting low-frequency slopes of 1 for log G'' and 2 for log G' have been reached within experimental uncertainty. The rubbery region and the approach toward a glassy response are indicated again.

In the past, experimenters have taken function values at the points of inflection in logarithmic plots of $J_R(t)$, $J'(\omega)$, and $G'(\omega)$ as measures of the rubbery plateau so that M_e could be calculated. It is desirable to point out that the inflection point of log $J_R(t)$ appears to give a value that is indistinguishable from that obtained from the integration calculation. This value for log J_N was estimated to be log $J_R(t)$ = −6.66 at log t/a_T = 1.02 whereas the values for log J' and log G' were −6.58 and −6.62 at log ωa_T's 0.40 and 1.00, respectively.

Loss Tangent. The logarithm of the loss tangent $(J''/J' = G''/G' = \tan \delta)$ of amorphous PP is shown in Figure 10 as a logarithmic function of the reduced circular frequency $\omega_r = \omega a_T$. At low frequencies the dominance of the viscous deformation is seen. The viscousless loss tangent, $(J'' - 1/\omega\eta)/J'$, is also shown. This parameter reflects the

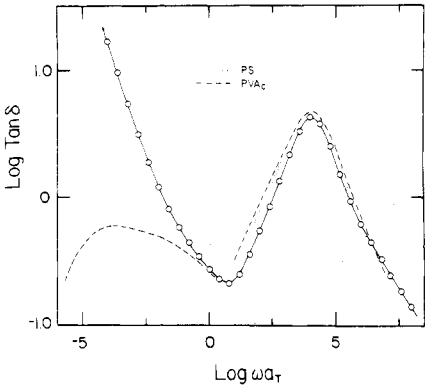

Figure 10. Logarithm of the loss tangent tan δ of amorphous polypropylene vs. the logarithm of the reduced circular frequency ωa_T. The dashed line is the viscousless loss tangent $(J'' - 1/\omega\eta)/J'$. The loss tangent curves for polystyrene and poly(vinyl acetate) are also shown in the molecular weight independent frequency range, shifted along the reduced frequency scale to match peak positions. T_0 for polypropylene is 25 °C.

long-time terminal peak of L and hence is sensitive to the molecular weight and its distribution.

The high-frequency peak of tan δ associated with the softening dispersion is surprisingly symmetrical and similar in shape and magnitude to the corresponding peaks for PS and PVAc, which are also shown in Figure 9, shifted to match the positions of the maxima. The PS curve is slightly higher over most of the frequency scale, and the PVAc curve appears somewhat broader. How significant these differences are is difficult to say. The relative magnitudes of the loss tangent peaks are in order of the rubbery plateau compliances J_N 2.21×10^{-7}, 2.82×10^{-7}, and 4.90×10^{-7} cm^2/dyn for polypropylene, poly(vinyl acetate), and polystyrene, respectively. The increasing peak loss is probably a consequence of the strength of the dispersion, $J_N - J_g$, since vinyl polymers with one side group on every other backbone carbon atom have close to identical narrow retardation spectra in the region of the glass-to-rubber softening dispersion. The value of J_N really determines the strength since J_g values differ little and $J_N > 10^3 J_g$.

Conclusions

A recent attempt has been made[49] to test the dependence of the entanglement rubbery plateau level $J_N = G_N^{-1}$ solely upon the "total length of chain contour per unit volume" νL (where ν is the number of chains per unit volume and L is the chain length) and the Kuhn step length $l = C_\infty l_0$. C_∞ is the characteristic ratio for the polymer and l_0 is the average length of the main-chain bonds. $C_\infty = \langle R^2 \rangle_\Theta / n l_0^2$, where $\langle R^2 \rangle_\Theta$ is the mean square chain end-to-end distance in a Θ solvent and n is the number of bonds per chain. G_N is the rubbery entanglement plateau modulus. The proposed relationship between the dimensionless interaction density $G_N l^3/kT$ and the dimensionless contour length concentration $\nu L l^2$ is

$$G_N l^3/kT = 0.010(\nu L l^2)^2$$

Using values of $C_\infty = 6.2$,[50,51] $l_0 = 1.54 \times 10^{-8}$ cm,[49] $\rho = 0.850$ g/cm^3,[11] and $G_N = 4.52 \times 10^6$ dyn/cm^2 for amorphous polypropylene, one obtains for $T = 298$ K, $G_N l^3/kT = 0.078$ and $\nu L l^2 = 3.4$, which places PP about 21% to the right of the line, well within the range of the scatter reported for Graessley and Edwards.

Successful apparent temperature reduction of the $J(t)$ curves measured over a range of 85 °C was achieved. However, extended viscosity measurements showed the reduction to be fallacious. In this sense and in the viscoelastic response in the softening dispersion, polypropylene is shown to be quantitatively close to polystyrene and poly(vinyl acetate) except for the rubbery plateau compliance. The conventional T_g was judged to be −14 °C.

Acknowledgment. This work was supported in part by the National Science Foundation, Engineering Division, Chemical and Biological Processes Program, under Grant No. CPE-8024713. We are grateful to J. B. Class of Hercules Inc. for providing the characterized polypropylene of low crystallinity, to L. J. Fetters of the Institute of Polymer Science, University of Akron, for GPC characterization of the studied fraction, and to S. Narayanan for assistance in the DSC determination of the T_g at the University of Pittsburgh.

Registry No. Polypropylene, 9003-07-0.

References and Notes

(1) M. Baccoredda and E. Butta, *Chim. Ind. (Milan)*, **40**, 6 (1958).
(2) J. A. Sauer, R. A. Wall, N. Fuschillo, and A. E. Woodward, *J. Appl. Phys.*, **29**, 1385 (1958).
(3) A. H. Willbourn, *Trans. Faraday Soc.*, **54**, 717 (1958).
(4) N. G. McCrum, *Makromol. Chem.*, **34**, 50 (1959).
(5) S. Newman and W. P. Cox, *J. Polym. Sci.*, **46**, 29 (1960).
(6) J. Van Schooten, H. Van Hoorn, and J. Boerma, *Polymer*, **2**, 161 (1960).
(7) H. A. Flocke, *Kolloid Z.*, **1980**, 118 (1962).
(8) E. Passaglia and G. M. Martin, *J. Res. Natl. Bur. Stand. (U.S.)* **68**, 519 (1964).
(9) B. Maxwell and J. E. Heider, *SPE Trans.*, **2**, 174 (1962).
(10) J. A. Faucher, *Trans. Soc. Rheol.*, **3**, 81 (1959).
(11) G. F. Natta, F. Danusso, and G. Moraglio, *Angew., Chem.*, **69**, 686 (1957).
(12) T. Hideshima, *Rep. Prog. Polym. Phys. Jpn.*, **5**, 103 (1962).
(13) G. F. Natta, F. Danusso, and G. Moraglio, *J. Polym. Sci.*, **25**, 119 (1957).
(14) M. L. Dannis, *J. Appl. Polym. Sci.*, **1**, 121 (1959).
(15) F. S. Dainton, D. M. Evans, F. E. Hoare, and T. P. Melia, *Polymer*, **3**, 286 (1960).
(16) J. J. Keavney and E. C. Eberlin *J. Appl. Polym. Sci.*, **3**, 47 (1960).
(17) E. Passaglia and H. K. Kevorkian, *J. Appl. Phys.*, **34**, 90 (1963).
(18) M. L. Williams, R. F. Landel, and J. D. Ferry, *J. Am. Chem. Soc.*, **77**, 3701 (1955).
(19) D. J. Plazek and J. H. Magill, *J. Chem. Phys.*, **45**, 3038 (1966).
(20) C. A. Russel, *J. Appl. Polym. Sci.*, **4**, 219 (1960).
(21) R. G. Quynn, J. L. Riley, D. A. Young, and H. D. Noether, *J. Appl. Polym. Sci.*, **2**, 166 (1959).
(22) M. Takayangi, *Mem. Fac. Eng., Kyushu Univ.*, **23**, 41 (1963).
(23) F. Danusso and G. Moraglio, *Makromol. Chem.*, **28**, 250 (1958).
(24) J. B. Kinsinger and R. E. Hughes, *J. Phys. Chem.*, **63**, 2002 (1959).
(25) A. Kotschkima and M. Grell, *J. Polym. Sci., Part C*, **No. 16**, 3731 (1968).
(26) D. J. Plazek, *J. Phys. Chem.*, **69**, 3480 (1965); *J. Polym. Sci., Part A-2*, **6**, 621 (1968).
(27) K. Ninomiya, *J. Phys. Chem.*, **67**, 1152 (1963).
(28) J. D. Ferry, L. D. Grandine, and E. R. Fitzgerald, *J. Appl. Phys.*, **24**, 911 (1953).
(29) E. Riande, H. Markovitz, D. J. Plazek, and N. Raghupathi, *J. Polym. Sci., Polym. Symp.*, **No. 50**, 405 (1975).
(30) F. Schwarzl and A. J. Staverman, *J. Appl. Phys.*, **23**, 838 (1952).
(31) D. J. Plazek, *Polym. J.*, **12**, 43 (1980).
(32) D. J. Plazek, *J. Polym. Sci., Polym. Phys. Ed.*, **20**, 729 (1982).
(33) J. D. Ferry, "Viscoelastic Properties of Polymers", 3rd ed., Wiley, New York, 1980.
(34) M. L. Williams, R. F. Landel, and J. D. Ferry, *J. Am. Chem. Soc.*, **77**, 3701 (1955).
(35) A. K. Doolittle, *J. Appl. Phys.*, **22**, 1471 (1951); **23**, 236 (1952).
(36) H. Vogel, *Phys. Z.*, **22**, 645 (1921).
(37) G. S. Fulcher, *J. Am. Chm. Soc.*, 8, 339, 789 (1925).
(38) G. Tamman and W. Hesse, *Z. Anorg. Allg. Chem.*, **156**, 245 (1926).
(39) S. J. Orbon, Ph.D. Thesis, University of Pittsburgh, 1978.
(40) E. N. da C. Andrade, *Proc. R. Soc. London, Ser. A*, **84**, 1 (1910).
(41) K. Van Holde, *J. Polym. Sci.*, **24**, 417 (1957).
(42) D. J. Plazek, W. Dannhauser, and J. D. Ferry, *J. Colloid Sci.*, **16**, 101 (1961).

(43) D. R. Reid, *Br. Plast.*, 2 (1959).
(44) D. J. Plazek, E. Riande, H. Markovitz, and N. Raghupathi, *J. Polym. Sci., Polym. Phys. Ed.*, 17, 2189 (1979).
(45) D. J. Plazek, *J. Colloid Sci.*, 15, 50 (1960).
(46) D. J. Plazek, V. Tan, and V. M. O'Rourke, *Rheol. Acta*, 13, 367 (1974).
(47) N. Raghupathi, Ph.D. Thesis, University of Pittsburgh, 1975.
(48) S. J. Orbon and D. J. Plazek, *J. Polym. Sci., Polym. Phys. Ed.*, 17, 1871 (1979).
(49) W. W. Graessley and S. F. Edwards, *Polymer*, 22, 1329 (1981).
(50) M. Kurata and W. H. Stockmayer, *Adv. Polym. Sci.*, 3, 197 (1963).
(51) J. B. Kinsinger and R. E. Hughes, *J. Phys. Chem.*, 67, 1922 (1963).

Screening of Hydrodynamic Interaction in a Solution of Rodlike Macromolecules

M. Muthukumar*

Department of Chemistry, Illinois Institute of Technology, Chicago, Illinois 60616

S. F. Edwards

Cavendish Laboratory, University of Cambridge, Cambridge, England CB3 0HE.
Received February 1, 1983

ABSTRACT: Using an effective medium argument, we show that the screening of hydrodynamic interactions has only a weak effect on the zero-shear-rate viscosity of a solution of rodlike molecules. The hydrodynamic screening length (ξ) varies with the monomer density (ρ) as $\xi \approx \rho^{-1/2}$, in contrast with $\xi \sim \rho^{-1}$ for the case of a solution of flexible chains under similar conditions.

Introduction

It is well-known[1] that for a dilute solution of long rodlike macromolecules the intrinsic viscosity ($[\eta]$) is proportional to M^2 if the hydrodynamic interaction is completely ignored (where M is the molecular weight of the rod). The incorporation[1-6] of hydrodynamic interactions leads to the familiar result $[\eta] \sim M^2/\ln M$. When the number density of the rods in the solution is increased, the hydrodynamic interaction between any two space points in the fluid is progressively screened. The concentration dependence of the screening is derived in this paper. We show that the specific viscosity, $(\eta - \eta_0)/\eta_0\rho$, is proportional to $M^2/\ln \rho$ in the high-concentration limit, where ρ is the monomer density and η and η_0 are the viscosities of the solution and solvent, respectively.

The analogous results for solutions of flexible chains are the following.[7,8] When hydrodynamic interaction is ignored, $[\eta] \propto M$. The incorporation of the hydrodynamic interaction leads to $[\eta] \propto M^{1/2}$. In the dense limit, where the hydrodynamic interaction is completely screened, $[(\eta - \eta_0)/\eta_0\rho] \propto \rho M$. Thus the hydrodynamic interaction plays a less pronounced role in the transport properties of solution of slender rods than in the case of flexible chains.

In the treatment of the transport coefficients of solutions of rods, it is necessary to introduce a cutoff at short distances.[1-6] However, it does not matter what this cutoff is since a proper solution is not yet available in this limit anyway. For simplicity, we consider the Riseman–Kirkwood–Auer model[3,4] for the rod which treats the rod as a line of $2n + 1$ beads separated by a step length l so that the length of the rod is $L = 2nl$. The length of the rod is taken to be very large compared to the diameter (d) of these beads, so that the beads can be treated to be point frictional sources. As mentioned above, any theoretical treatment requires a cutoff at short distances along the rod. We choose the step length l to be this cutoff.

We have deliberately ignored the entanglement effect[9-11] between the various rods, as we are interested here in finding how weak the effect of hydrodynamic interaction is on the transport properties of solutions of rods and what the concentration dependence of the hydrodynamic screening length is. Since the rods begin to get entangled for $c > L^{-3}$ (c = number density of rods), the formulas derived below are valid for L such that $d \ll L \ll c^{-1/3}$. Thus it may be possible to get to the screened regime for a solution of short but thin rods. Although there has been an earlier attempt[12] at describing the hydrodynamic interaction in an entangled semidilute solution of rods, the problem addressed here is even simplier but basic.

The important results derived in this paper are summarized as follows:

(i) The reduced viscosity is given by

$$(\eta - \eta_0)/\eta_0 = (\pi/12)cL^3/\ln (L/l) \qquad \text{low } c$$

$$(\eta - \eta_0)/\eta_0 = (\pi/12)cL^3/E_1(l\xi^{-1}) \qquad \text{high } c \qquad (1)$$

where E_1 is the exponential integral.[13]

(ii) The screening length ξ appearing in eq 1 is given by

$$\xi^{-2}E_1(l\xi^{-1}) = 3\pi cL \qquad (2)$$

Basic Equations

The fluid in the absence of the suspended rods is taken to obey the linearized Navier–Stokes equation (in the steady-state limit).

$$-\eta_0\nabla^2\mathbf{v}(\mathbf{r}) + \nabla p(\mathbf{r}) = \mathbf{F}_e(\mathbf{r}) \qquad (3)$$

Here $\mathbf{v}(\mathbf{r})$ is the velocity field at any space point $\mathbf{r}$, p is the pressure, η_0 is the shear viscosity of the solvent, and $\mathbf{F}_e(\mathbf{r})$ is the external field driving the fluid flow. Assuming that the fluid is incompressible, this equation can be written as an integral equation in terms of the familiar Oseen tensor $\mathbf{G}_0$.

$$\mathbf{v}(\mathbf{r}) = \int d\mathbf{r}'\, \mathbf{G}_0(\mathbf{r} - \mathbf{r}')\cdot\mathbf{F}_e(\mathbf{r}')$$

$$\mathbf{G}_0(\mathbf{R}) = (1/8\pi\eta_0|\mathbf{R}|)(1 + \mathbf{RR}/|\mathbf{R}|^2) \qquad (4)$$

The long-ranged hydrodynamic interaction present in a solvent as given by the Oseen tensor is altered by the presence of rods, and this modification is the origin of the screening of the hydrodynamic interaction. The extent of the screening as a function of the polymer density is derived below.

0024-9297/83/2216-1475$01.50/0